

Experimental investigation of hysteretic stiffness related effects in contact-type nonlinearity

A. Klepka  · K. Dziedziech · J. Spytek ·
J. Mrówka · J. Górski

Received: 13 February 2018 / Accepted: 28 October 2018 / Published online: 14 November 2018
© The Author(s) 2018

Abstract The paper presents experimental works related to contact nonlinearities. The research is focused on effects derived from hysteresis stiffness characteristics and vibro-impacts generated during the relative movement of two surfaces. The modeling of the contact nonlinearities was divided in two parts. First, the parameters of the system were identified based on modal analysis test. Next, the model was created and verified with experimental data. The experimental works were performed on steel samples with prepared contact surfaces. Electromagnetic shaker was used to produce relative motion between surfaces in contact. The response of the system was acquired by non-contact laser vibrometer. Both displacement and velocity of vibration were measured. Additionally, the impedance head measures the force and acceleration. The experimental data were used to validate the created models.

Keywords Contact nonlinearities · Contact model · Structural dynamics · Hysteresis stiffness

1 Introduction

The relative motion of two surfaces with adhesion is the process where a lot of nonlinear mechanism occurs. A lot of studies on different friction laws, different contact stiffness and different contact model have been reported, but there are still a lot of questions and hypotheses related to nonlinear mechanisms of contact. Although there are many unexplained contact mechanics phenomena, many applications based on nonlinear contact effects are used for diagnostic purposes. One of the method utilizes contact related nonlinear phenomena is nonlinear acoustics. Over the last 20 years, these methods are intensively developed for damage detection and localization. There are a lot of applications where nonlinear effects are used to identify and localize faults and damages [1–5]. This technique based on identification of nonlinear effects generated due to contact damage related nonlinearities. The effects are produced when the two types of excitation—low and high frequency—are introduced to the structure simultaneously. Then, the interaction of contact-type damage (e.g., fatigue crack or delamination) excited by low-frequency monoharmonic excitation with high-frequency acoustic wave results in different nonlinear product, observed in the response spectra. This can be signal modulation [6–8], higher and sub-harmonics [9–11], frequency shift when excitation amplitude increase [11, 12], frequency mixing [13], modulation transfer (Luxembourg-Gorky effect) [14, 15], memory effects [9] and many others [16–19].

A. Klepka (✉) · K. Dziedziech · J. Spytek · J. Mrówka ·
J. Górski
Department of Robotics and Mechatronics, AGH
University of Science and Technology, Al. Mickiewicza
30, 30-059 Kraków, Poland
e-mail: klepka@agh.edu.pl

The above-mentioned phenomena can be related to material nonlinearities or non-symmetric thermoelastic behavior of interfaces (e.g., contact-type damage). There are a lot of works where above-mentioned effects were used for structural damage identification in metallic structures [4, 7, 15, 19], composites [20–25], rocks [11] and a lot of different materials. The main conclusion of most of the works on this method is that nonlinear acoustic techniques are very sensitive and can detect damage in very early stage. This is because damage related nonlinearities produce significant effects in signal response. According to the literature, the damage-induced nonlinear mechanisms can be divided into three groups. The first is atomic scale where intrinsic elastic nonlinearity due to anharmonicity of interatomic potential [3], non-friction and non-hysteretic dissipation locally enhanced by thermoelastic coupling [25], hysteresis in stress–strain [26], stick-slip friction between crack surfaces or adhesion hysteresis [27] can be observed. The second is mesoscopic scale where crack induced nonlinearity (variation in elastic moduli) [27], Hertzian type nonlinearity (contact between crack surfaces) [28], local stiffness reduction leading to natural frequency shift [5] or bi-linear stiffness (closing–opening crack) [29] can occur. The last one is macroscopic scale and includes clapping mechanism [30] and wave modulation due to impedance mismatch (discontinuity due to closing–opening crack) [31]. Beyond the problems associated with the determination of nonlinearity sources, additional difficulties arise in this kind of research. Structures tested are usually elements with a complex shape. This generates problems because in many cases these elements themselves mask contact related (e.g., resulting from fatigue damage or delamination) nonlinear effects. One of the reason of that are linear and nonlinear structural components resulting from the construction of the structure, specific boundary conditions and impact induced structural components. This type of self-generating impacts causes wide-band excitation of the structure, whereby the signal response also includes high-frequency components related to structural dynamics [32–34]. Despite the multitude of phenomena and the possibility of applying nonlinear methods to many types of structures with contact-type damage, there are many unresolved problems. The first is related to ambiguity because the different nonlinear mechanism can be manifested by the same effects. Additionally, these mechanisms can occur simultaneously and modify structural response. This results in

the problems of modeling contact-type damage. The second problem is related to experimental validation of proposed model. It is very often hard to measure the physical quantities generated as effects of nonlinear mechanisms. For these reasons, many theories about dynamic phenomena in contact-type damage remain only hypotheses. In spite of these problems, nonlinear acoustics still remain attractive in the case of detection and localization of contact damage. Understanding of nonlinear mechanisms associated with the contact phenomenon may contribute to the further development of nonlinear techniques and can help to implement it in more engineering application.

The inspiration for elaborating the model with hysteresis stiffness and impact were phenomenon occurring in vibro-acoustic modulation tests described widely in many works [3, 16]. It should be noted that works in this field are mainly experimental. There is no model that would allow a clear explanation of nonlinear effects resulting from the interaction low-frequency excitation, ultrasonic wave and contact interface. The paper focus is on the elaborating model with hysteresis stiffness, vibro-impacts and experimental validation of the proposed model. In this paper only low-frequency excitation is investigated.

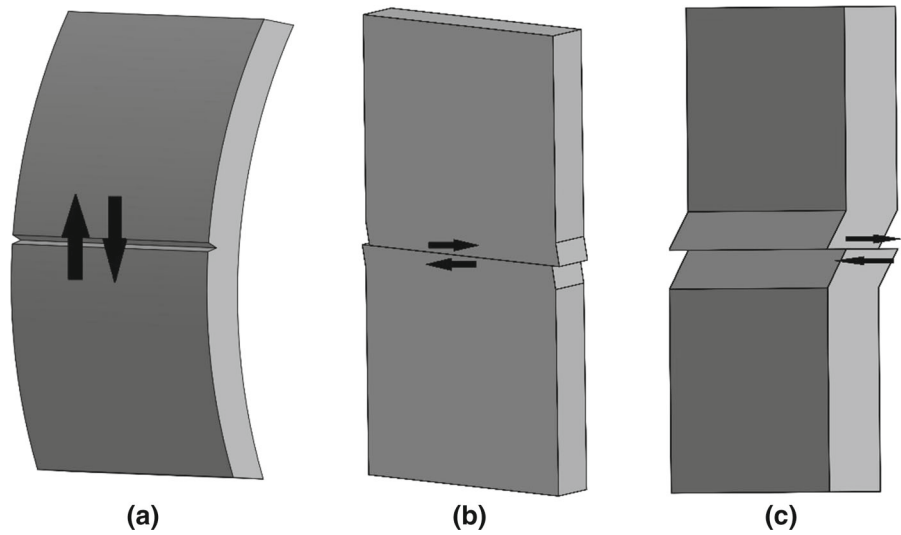
The remaining part of the paper is organized as follows. Section 2 contains theoretical background on stiffness characteristics related to contact. Section 3 the assumed numerical model is presented. In Sect. 4 numerical model is validated with experimental data. The discussion of results is also provided in that section. The paper is concluded in the last section.

2 Theoretical background

The most of delamination's or fatigue cracks in engineering structures have contact nature. When the structure vibrates with given frequency, the different types of contact can occur. In general, three different crack modes are expected:

- Closing–opening action, where the crack faces move apart from each other.
- Sliding action, where the crack faces slide relative to each other (the movement is perpendicular to the crack leading edge).
- Tearing action, where crack faces move relative to each other in direction parallel to crack leading edge.

Fig. 1 Three basic contact modes: **a** closing–opening mode, **b** sliding mode, **c** tearing mode



Schematically, these contact modes are presented in Fig. 1.

For the first mode (closing–opening action), the bi-linear stress–strain relation is expected. This is due to fact that the structure stiffness is higher for the compression, than for tensile phase. The bi-modular contact caused by structure vibration results in pulse type modulation of material stiffness. Then, the harmonics with amplitude modulated by *sinc* function of fundamental frequency are expected in the response spectra. Such behavior is often called “clapping” mechanisms and can be described using piecewise stress–strain relation [35]

$$\sigma = C^{\text{II}} \left[1 - H(\varepsilon) \left(\frac{\Delta C}{C^{\text{II}}} \right) \right] \varepsilon \quad (1)$$

where σ is stress, ε is strain, $H(\varepsilon)$ is unit step Heaviside function, C^{II} is linear stiffness and ΔC is described by formula [35]

$$\Delta C = \left[C^{\text{II}} - \left(\frac{d\sigma}{d\varepsilon} \right) \right] \quad (2)$$

for $\varepsilon > 0$. Figure 2 presents bi-linear stiffness characteristic and example of response spectra for “clapping” contact.

For the other two modes of contact, the different stress–strain characteristics are expected. There are mechanical diode effect and hysteretic stress–strain relation. If the amplitude of relative displacement between contact surfaces is low, the motion is lim-

ited to micro-slip mode due to surface roughness. The interactions of following asperities produce the friction forces and prevent surfaces from sliding. In this case, the symmetrical stress–strain relation occurs and only odd harmonics are generated. Due to pulse type stiffness modulation, the amplitude of the following harmonics is also modulated by *sinc* function (Fig. 3).

The last contact type is stick and slip mode. When the harmonic excitation is applied to two non-bonded surfaces and resulting strain is strong enough to change friction from static to kinematic then the hysteretic stress–strain relation is expected. In this case, the contact stiffness value changes twice per cycle from C_s (for stick phase) to zero (for slide phase) according to formula [36]

$$C(t) = \frac{C_s}{2} \{ 1 - \text{sign}(\dot{\varepsilon}) \text{sign}[\varepsilon + \text{sign}(\dot{\varepsilon}) \varepsilon_1] \} \quad (3)$$

By integration Eq. (3) with respect to time, the σ can be determined as a function of ε [36]

$$\sigma(t) = C(t) \varepsilon(t) + C(t) \varepsilon_1 \text{sign}(\dot{\varepsilon}) + \frac{C_s}{2} (\varepsilon_0 - \varepsilon_1) \text{sign}(\dot{\varepsilon}) \quad (4)$$

Since the stress–strain characteristic remains symmetrical, only odd harmonic are generated in the response spectra. The amplitudes of the following harmonics are also modulated by *sinc* function, but amplitude ratios of the following harmonics are different than for micro-slip mode. Figure 4 presents an example of stress–strain characteristic for hysteresis nonlinearity.

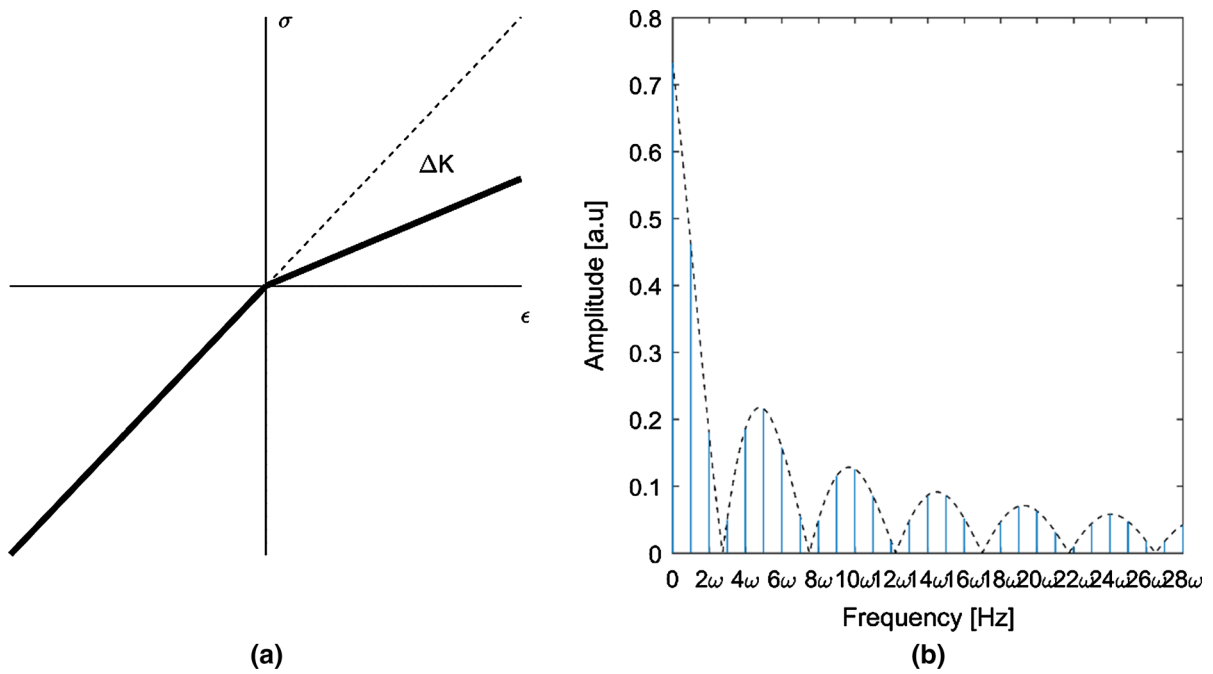


Fig. 2 **a** Stress–strain characteristic for bi-linear stiffness function; **b** example of corresponding response spectra

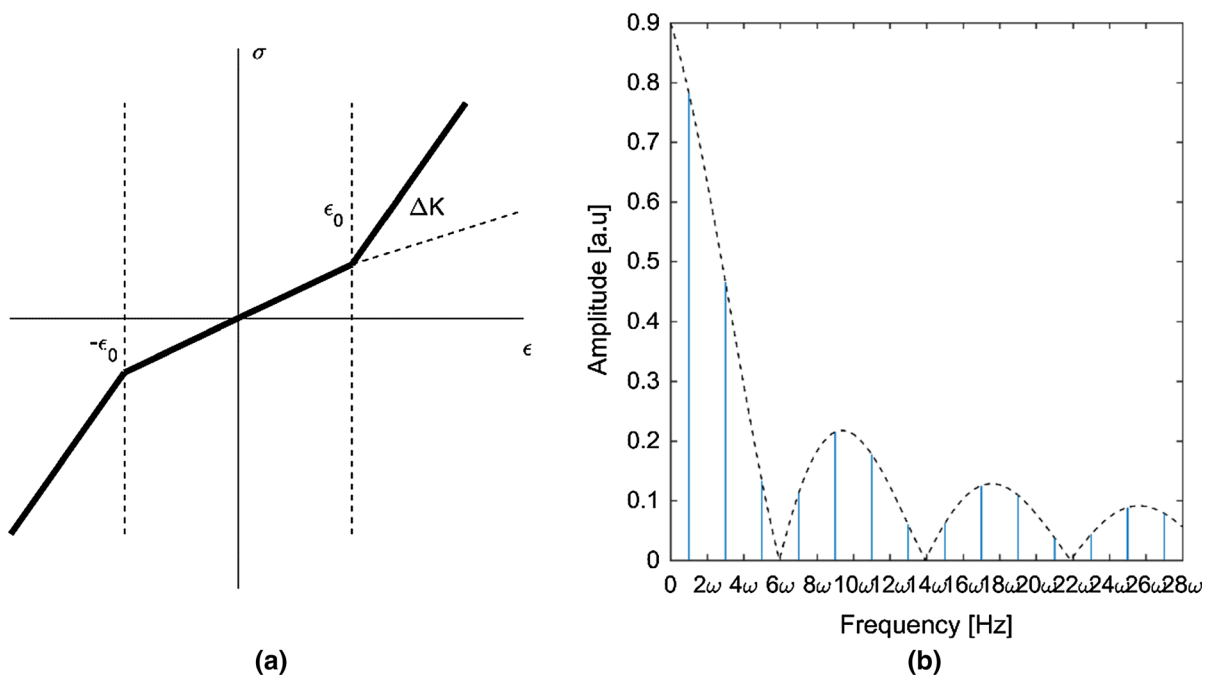


Fig. 3 Stress–strain characteristic for micro-slip mode **(a)** and expected spectrum of the response signal **(b)**

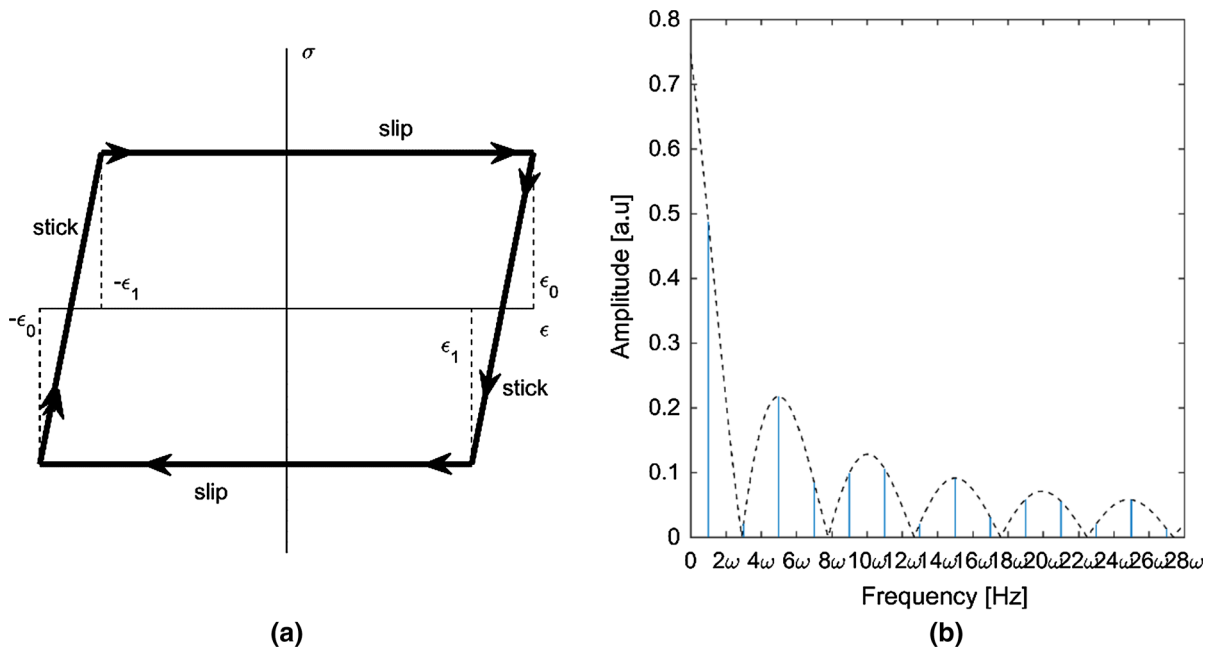


Fig. 4 **a** Stress–strain characteristic for stick-slip mode; **b** example of corresponding response spectra

The presented above stress–strain characteristic are of course ideal. It means, for example, that after every loading and unloading cycle, structure returns to the same state at the same point. For real structures, the characteristics can be modified due to additional phenomena like cyclic hardening and creeping. The real hysteretic characteristics can also deviate from the theoretical and can change for example depending on the strain rate sign.

The complexity of phenomena occurring in presented types of contact can result from many factors. It can be:

- the different dimensions of the contact (small for thin fatigue cracked plate and large for delaminated composite materials)
- the impulse excitation of the structure by roughness induced vibration
- the time-varying size of the contact area due to low and high frequency excitation
- the friction and adhesion forces acting at the contact interface and provide micro-slip and stick and slip processes
- the strain and temperature dependence of material properties.

All of the above-mentioned phenomena can cause different distortion in stiffness characteristics, including non-symmetry. Knowledge on the nonlinear phenomena occurring in the case of contact is important not only from the scientific point of view. Many damage detection methods are based on the effects produced by nonlinear mechanisms related to contact. Process of extraction of nonlinear components from signal response is complicated because very often is impossible to define where the effect should appear at the spectra. Additionally, the nonlinear damage detection methods are very sensitive for nonlinearities coming from other than damage related sources like nonlinearities of measurement chain, boundary conditions or material nonlinearities. One of the main problem in such cases is to separate damage and non-damage related nonlinear sources.

3 Numerical model

Numerical model description

This section provides simulation of numerical model with amplitude dependent stiffness model. This model

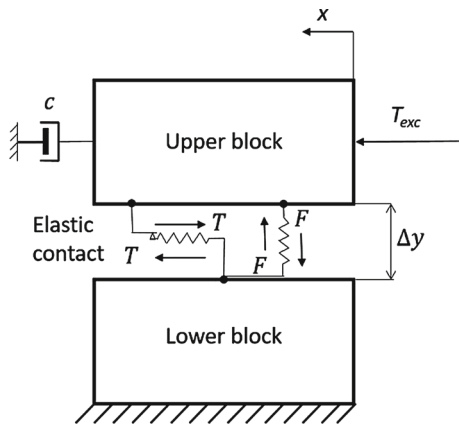


Fig. 5 Scheme of the investigated model

is implemented as 1DOF lumped parameter system presented in Fig. 5.

Due to the hysteretic stiffness, expected behavior is such that for the low excitation level, when the displacement will be in range of stick motion, the overall behavior will be different than in case of high excitation level, when the displacement will be in micro-slip and stick and slip motion. Additionally, when the motion will change from stick to slip phase, the assumed roughness induced impact is introduced to generate additional components related to the structure transfer function. The time-dependent system equations in tangential direction are

$$m\ddot{x} + c\dot{x} + k_Lx + k_Px + k_Hx + T = F_{exc} \quad (5)$$

where x , \dot{x} and \ddot{x} are displacement, velocity and acceleration in tangential direction respectively, k_L is linear stiffness of the system and F_{exc} is excitation force

$$F_{exc} = f_0 \sin(\omega t) \quad (6)$$

The k_P represents piecewise linear stiffness described by formula (according to Fig. 5.)

$$k_P = \begin{cases} k_1 & \text{for } x \leq x_{k1} \\ k_1 + k_2 & \text{for } x > |x_{k2}| \end{cases} \quad (7)$$

When $x \geq |x_H|$ then the hysteresis stiffness is introduced. The friction force T related to the contact force (vertical) is assumed as

$$T = \mu(\Delta\dot{x}) F \quad (8)$$

The normal contact force F is given by

$$F = k_C \Delta y H(\Delta y) \quad (9)$$

where y is displacement in vertical direction and Δy is displacement difference in vertical direction between upper and lower steel blocks

$$\Delta y = y_{upblock} - y_{loblock} \quad (10)$$

and k_C is contact stiffness parameters. $H(y)$ is Heaviside function and prevents the upper block to be lifted when Δy is negative. The displacement in vertical direction for upper block is calculated using Green's function (convolution of impulse response and contact force [37])

$$y_{upblock} = -F * g_{upblock} \quad (11)$$

For stiffness characteristics, the following scenarios are assumed. For low excitation level ($x > |x_{k2}|$), the piecewise stiffness characteristics is used (micro-slip, without vertical displacement). When amplitude of excitation reach assumed level ($x \geq |x_H|$), then the stiffness characteristic become hysteresis (Fig. 6) and additionally the impulse response of the structure is also included [according to Eq. (9)]. The displacements x_{k2} and x_H have been identified based on experimental data. Figure 6 presents stiffness characteristics of the investigated model.

The simulation was prepared in Matlab/Simulink environment, sampling frequency was 50 kHz, and total simulation time was 10 s. Schematic diagram of the model used is presented in Fig. 7.

4 Experimental setup

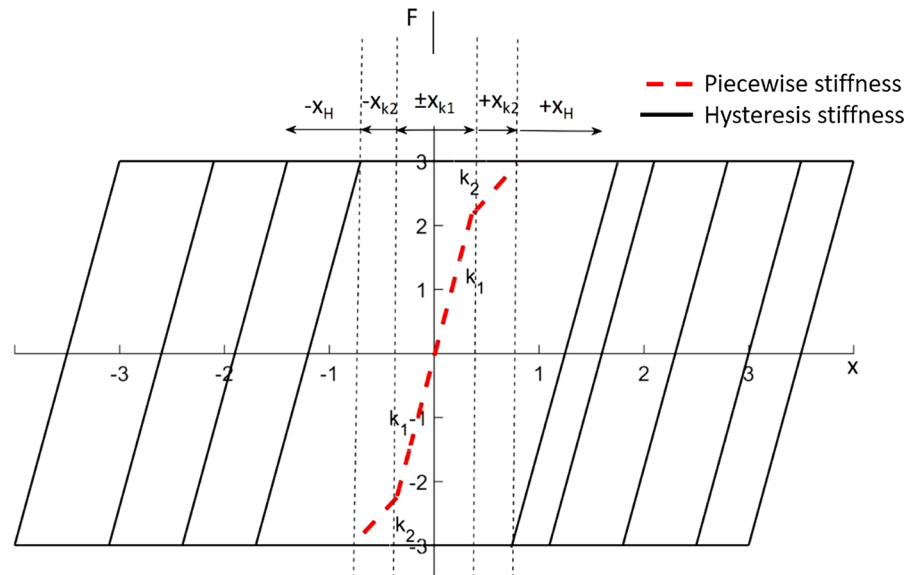
Description of the test samples

Two test samples made from C45 steel were prepared for testing. The overall dimensions of the test sample are $40 \times 40 \times 45$ mm with the contact surface of the area 10×10 mm. The contact surfaces are grounded with a sand paper with the grit size P40 to obtain rough surface. Figure 8 presents sample used in test.

Analysis of transfer function of the system

To pre-identify the parameters of the analyzed system, the modal analysis test was carried out. The investigated object has been freely suspended and piezo-

Fig. 6 Stiffness characteristic of the investigated model



electric actuator NOLIAC NAC 2013 is attached to object to excite the structure in high-frequency regions. Excitation signal was a chirp signal with frequency from 5 to 20 kHz. Fourier transform of the signal is shown in Fig. 9 with blue solid line. The three modes have been identified based on Frequency Response Function (FRF). For this modes damping ratio (using half-power method) and natural frequency has been estimated and the results are summarized in Table 1. These modes have been introduced to the model. The comparison of FRF for both numerical model and tested sample for the same excitation parameters is presented in Fig. 9.

It is worth noting that the estimated parameters were used in the simulation as initial parameters. Due to boundary conditions during the test, the values of frequency and damping can significantly change. In subsequent stages, they were tuned on the basis of experimental data.

Test rig description

In order to investigate phenomena related to the nonlinear stiffness contact, an experimental setup is created. It consists of modal shaker K2007E01 as an excitation source. One sample was mounted at the end of threaded rod connected to the shaker and the other was firmly attached to the steel base plate. In this configuration, the relative motion in a single axis could occur between the samples. The top sample is loaded by an extender mass 200 g. The experimental setup is shown in Fig. 10a.

The data measurement was conducted using impedance head PCB 288D01 to obtain acceleration and force data and the Doppler laser vibrometer to record displacement and velocity data. The excitation signal is supplied by the means of Agilent 33500B Series generator controlled by Matlab script and the acquisition was performed using Polytec PSV software. Sampling frequency is 51.2 kHz with total acquisition time 9 s. A series of measurements are conducted with sine excitation with frequency ranging from 10 to 500 Hz, with step of 10 Hz, so in total 50 measurements are obtained. Amplitude is linearly increasing during each experiment, to observe the nonlinear behavior.

Results and discussion

At first, time domain signals are analyzed. Detailed analysis is limited to signal that was excited with frequency 10 Hz. Displacement and velocity signals are analyzed as shown in Figs. 11 and 12, respectively. It is observed that the entire motion could be divided into two parts, i.e., up to 2.6 s when the displacement amplitude increase very slowly, and above 2.6 s when displacement linearly increases. Figure 13 presents comparison of displacement signals zoomed at this time interval.

To analyze the particular stick and slip phase, the time domain signal was zoomed to one period of motion and is presented in Fig. 14. Then, the one period window of the signal was investigated.

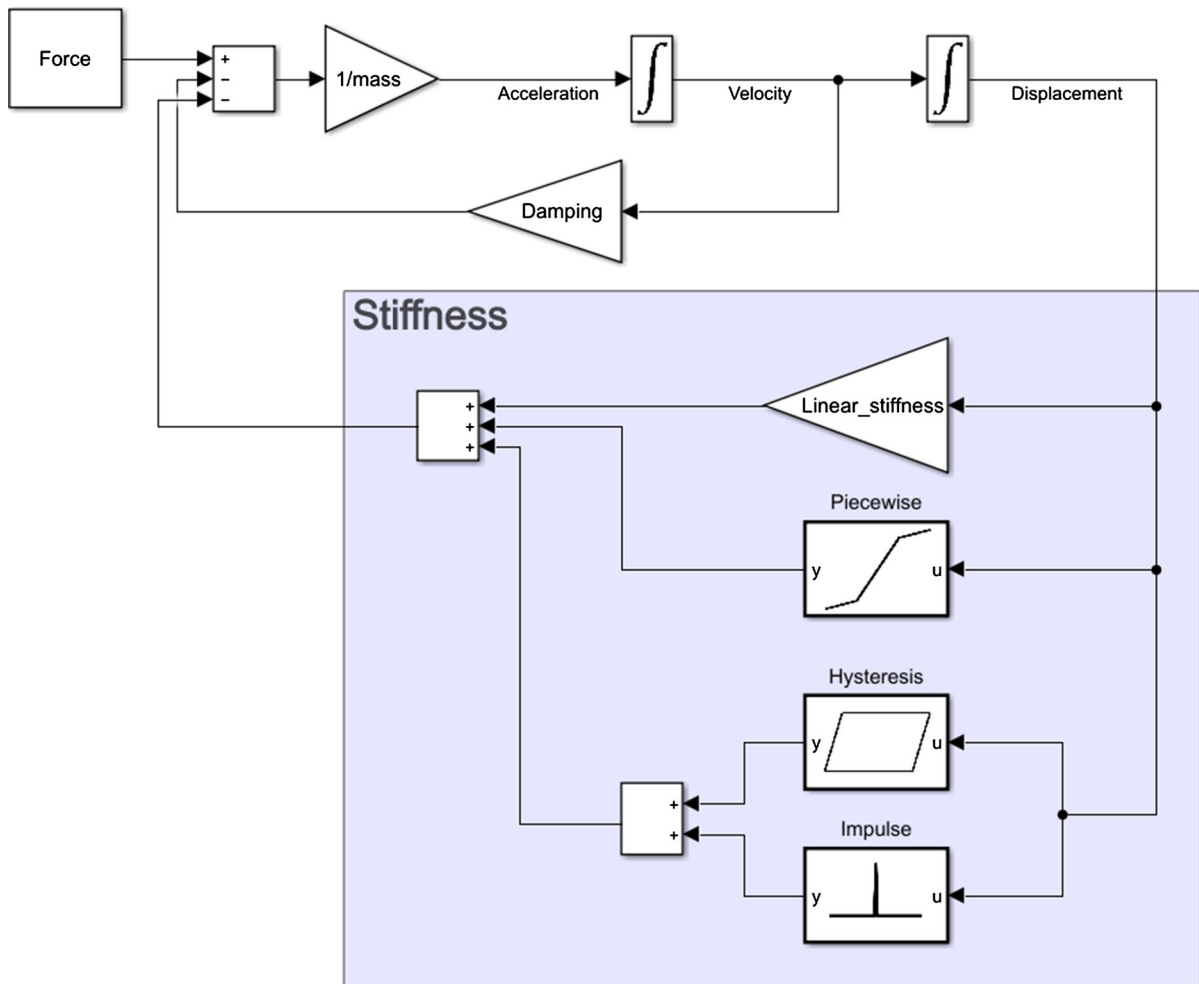


Fig. 7 Schematic diagram of nonlinear model with hysteresis stiffness

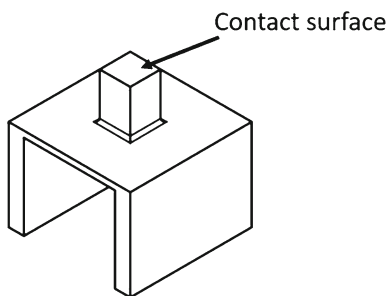


Fig. 8 Investigated sample

The four different motion phases are visible when Fig. 14 is analyzed—two for stick and two for phase motion. Additionally, the high-frequency structural components can be observed (Fig. 15a). The nature

of this component is different than in the numerical model. The reason for this may be that the measurement data is collected at a certain distance from the contact interface. This means that there is a transfer function between the contact area and the measuring point that can modify the response signal. The model does not take into account the geometry of the structure.

In order to analyze the high-frequency components (related to the vibro-induced impacts), spectrograms for the velocity data have been calculated as shown in Fig. 15. It is clearly shown that at time 2.4 s, there are additional components visible in high-frequency range for both numerical example and experimental data. Additionally, for experimental data, the harmonics of the structural modes are also visible.

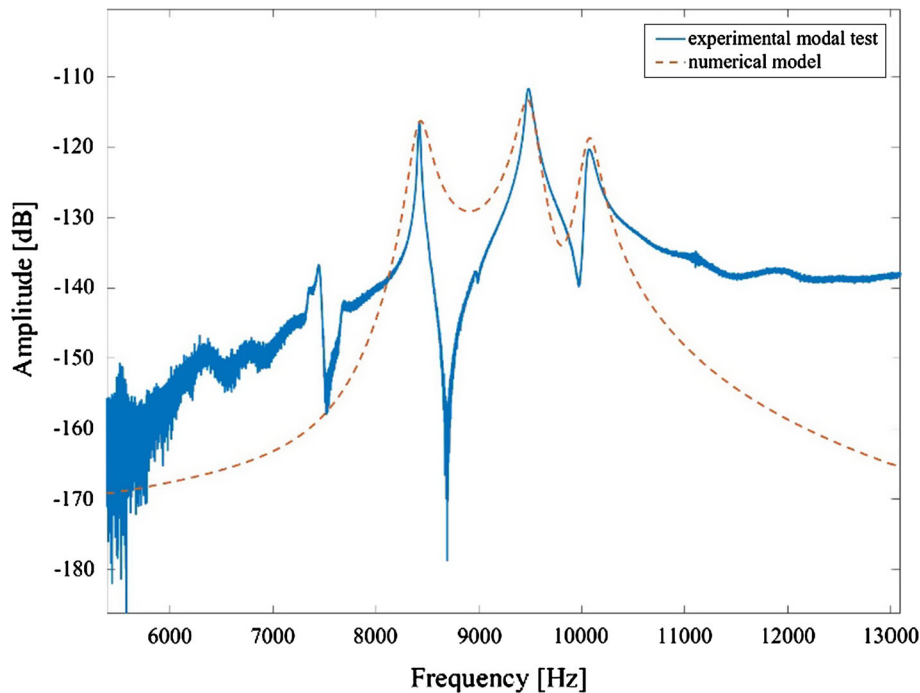


Fig. 9 Frequency response function for numerical model (red dashed line) and experimental data (blue solid line). (Color figure online)

Table 1 Frequency and damping ratio values for identified high-frequency modes

Mode number	Frequency (Hz)	Damping (%)
1	8120	0.07
2	9393	0.05
3	10,225	0.03

In order to visualize the difference between the frequency content of both phase of motions, Fourier transform has been calculated. For the piecewise stiffness part of the signal in vicinity of time $t = 0-2$ s is considered. For the hysteretic stiffness part of the signal in vicinity of time $t = 3-9$ s is considered. Figures 16 and 17 present comparison of spectra calculated for model and experimental data.

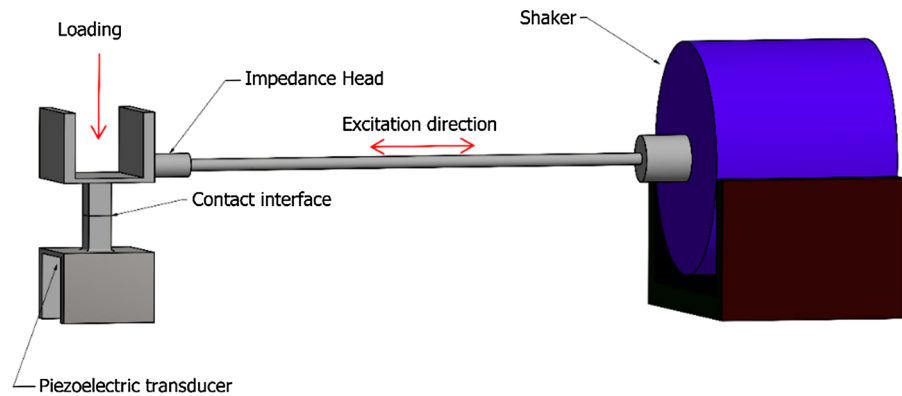
It can be also noticed that there is a good agreement between model and experimental data results. For both the two phase of motion can be clearly recognized. The frequency components are very similar when Figs. 16 and 17 are compared. Moreover, the experimental data includes additional components (about 20 kHz), probably related to harmonics of natural frequency. This problem is not investigated in this paper.

Frequency dependence of motion types

It is shown in previous section that the type of nonlinearities present actually depend on the type of motion occurring, and this is related to relative displacement of two surfaces in contact. As it is shown in Fig. 14a, there are different phases of motion that depend on the value of relative displacement, i.e., additional high-frequency components appear in the signal, when certain displacement threshold value has been crossed, as seen in Fig. 15b.

In many examples of nonlinear acoustic tests, the effects associated with contact depend on excitation frequency. To verify this, the analyses have been performed to find the threshold level at which the high-frequency components appear in the response signals depending on the low-frequency excitation frequency. In the investigated model, the constant value of displacement specifying the change in motion phase has been assumed. For this purpose, the experiment with set of excitation frequency values has been performed. The values were changed from 10 to 500 Hz with step 10 Hz. The amplitude of excitation was assumed as in previous experimental works. Next, the displacement data

Fig. 10 Experimental test rig: **a** schematic view and **b** photo



(a)



(b)

were used to find the moment when the high-frequency structural components appear at the signal spectra. Figure 18a presents the characteristic calculated for given frequency range. This figure shows that the moment of motion change is different for the whole frequency range and it is not constant.

Theoretical model assumes constant value of ε_1 (according to Fig. 4), on the basis of which type of motion changes, while the analysis of Fig. 18a suggests frequency dependent behavior. To investigate this problem, the additional modal analysis test was performed to find low-frequency structural components. Figure 18b presents FRF (red solid line) for frequency range up to 500 Hz. When the displacement threshold and FRF are compared, then the consistency of both can be noticed. It follows that the structural resonance

of the sample (about 150 Hz) affects the moment of motion changes. Generated resonant vibrations cause additional displacement and in this way changes the moment of appearance of high-frequency structural components. Hence, the conclusion that in order to properly adjust the excitation level in nonlinear acoustics tests, both high- and low-frequency structural components should be taken into account.

5 Conclusions

Experimental and numerical investigation of hysteretic stiffness for contact-type nonlinearity was presented. The numerical model with non-symmetrical, amplitude dependent hysteresis stiffness was developed. The

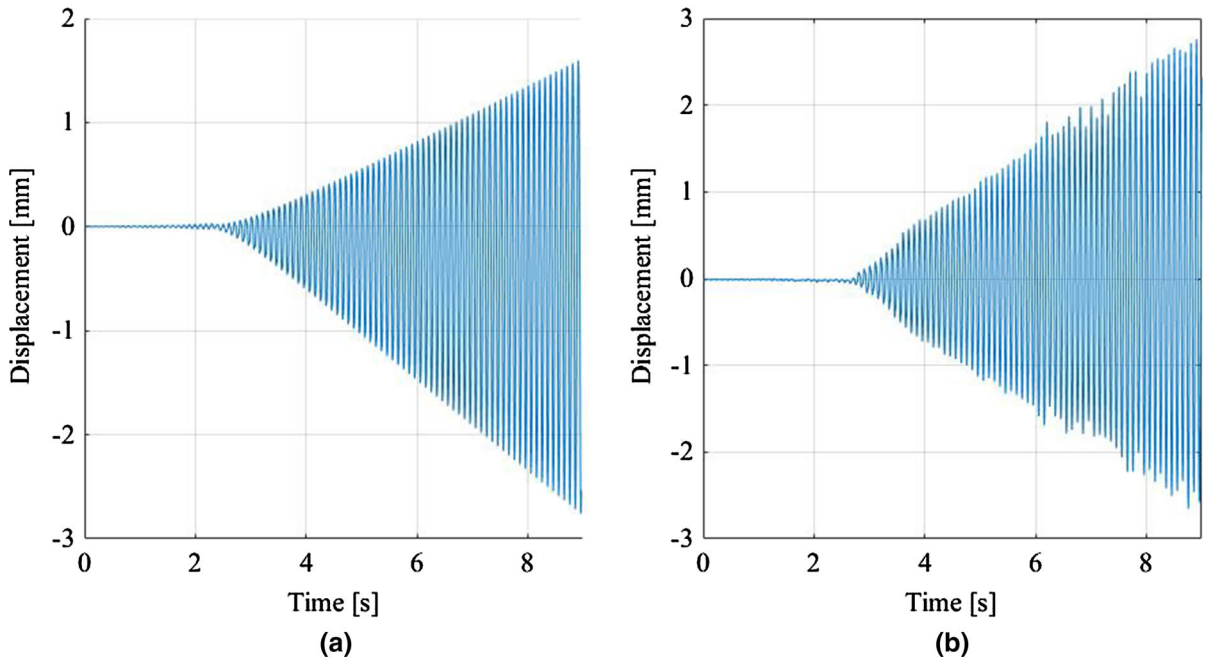


Fig. 11 Time domain signals of displacement from numerical model (a) and experiment (b) with excitation frequency 10 Hz

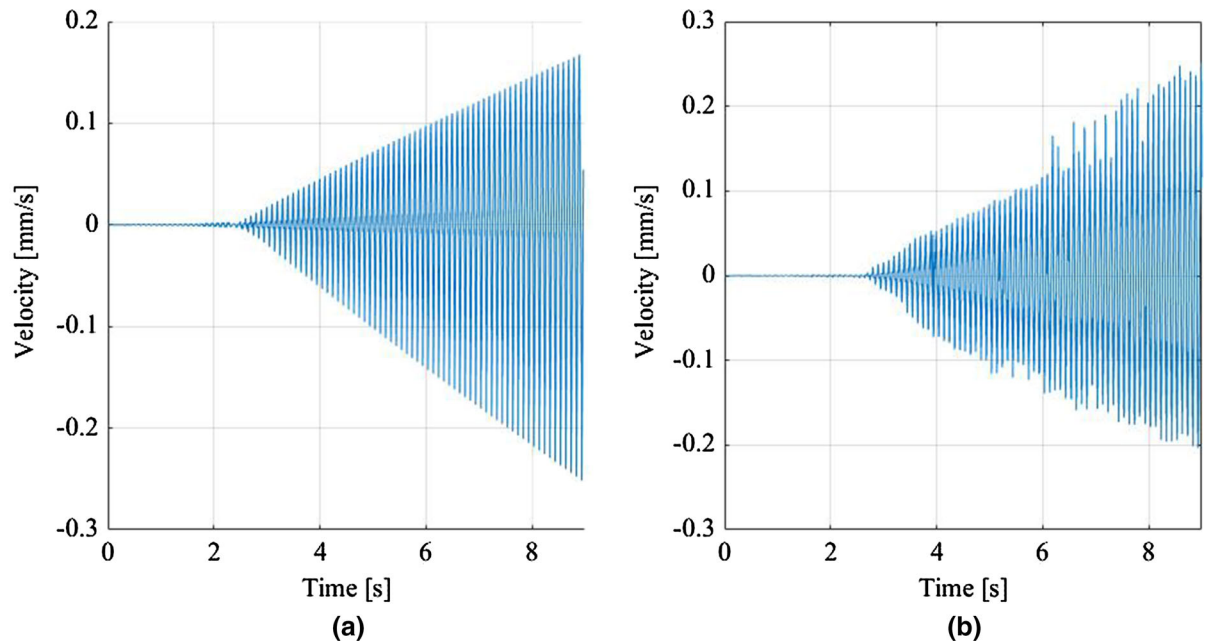


Fig. 12 Time domain signals of velocity from numerical model (a) and experiment (b) with excitation frequency 10 Hz

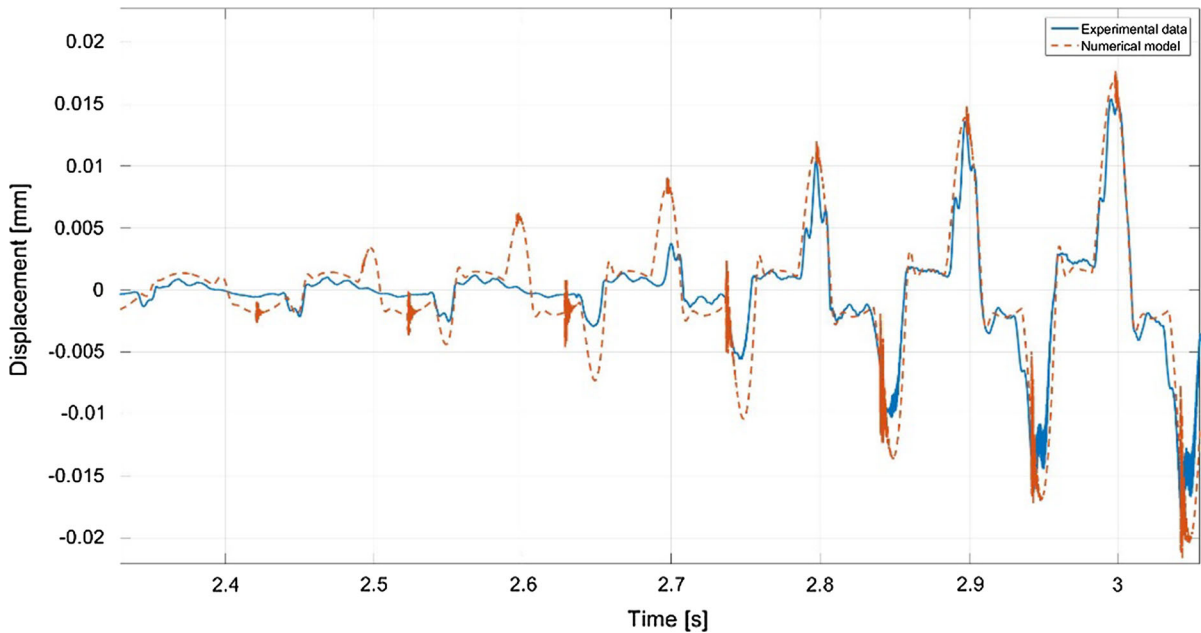


Fig. 13 Zoomed time domain displacement signals from numerical model (red dashed line) and experiment (blue solid line) with excitation frequency 10 Hz. (Color figure online)

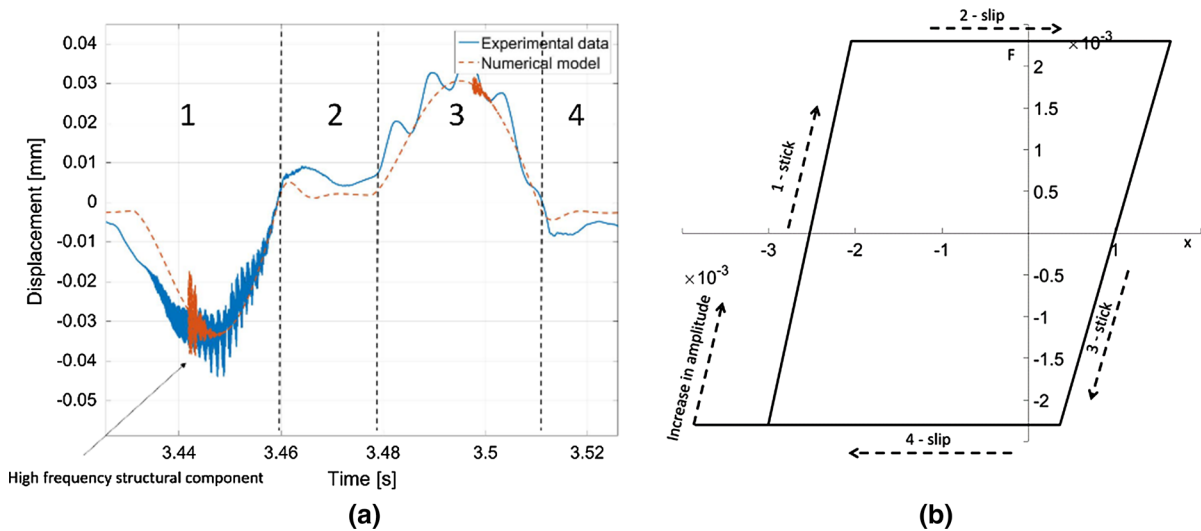


Fig. 14 One period of the time domain response signal (a) and corresponding stiffness characteristics for different motion phases (b)

two steel samples with contact were used for experimental work. The monoharmonic signals with a linearly increasing amplitude were used for both cases as excitation. Additionally, the structural dynamics was included in numerical model. The study involved the analysis of two motion types: micro-slip and stick and slip. The experimental results demonstrate that the dis-

placement level caused motion phase change is closely related to the resonance vibrations of the structure. For these reasons, it is important to consider the appropriate frequency of excitation when nonlinear effects related to different types of motion/contact are analyzed. The time and frequency domain analyses confirm that inclusion of additional high-frequency struc-

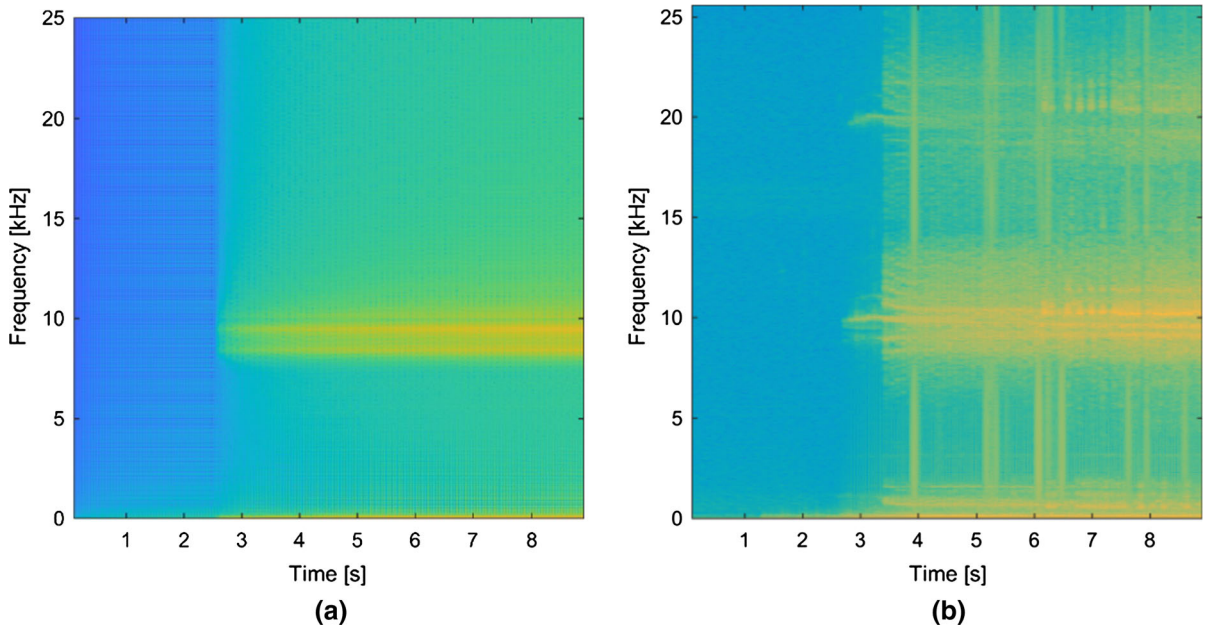


Fig. 15 Spectrograms of the velocity signals from numerical model (a) and experimental data (b)

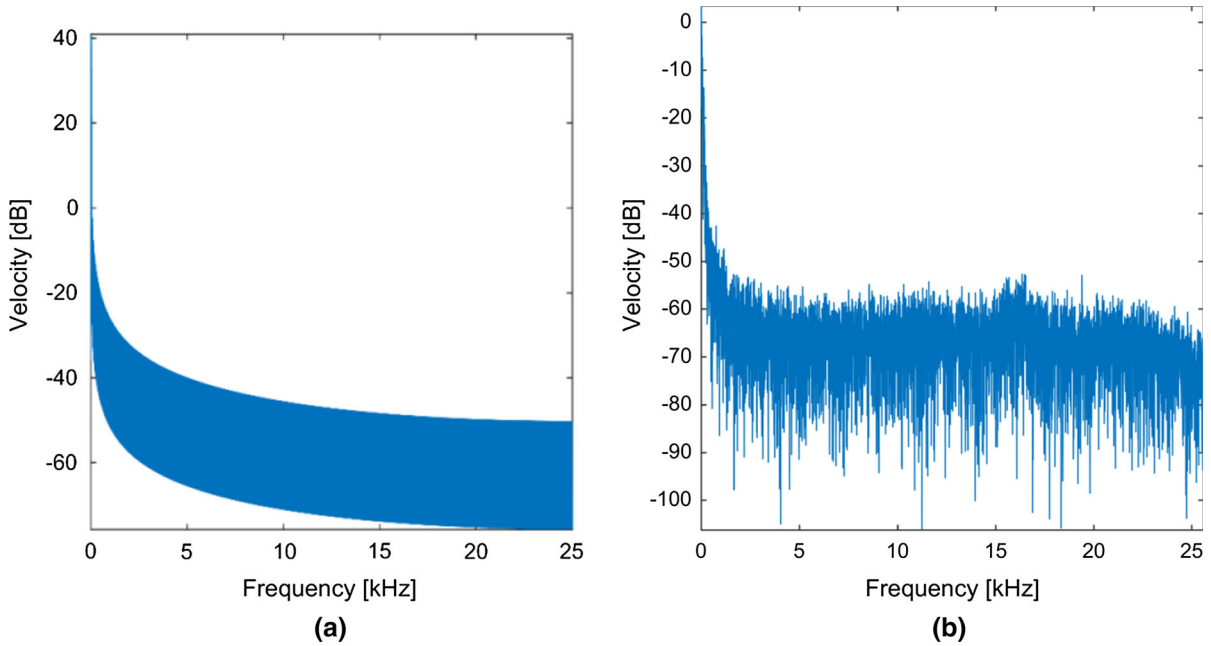


Fig. 16 Fourier transform of velocity signal from model (a) and experimental example (b) at time interval $t = 0\text{--}2$ s

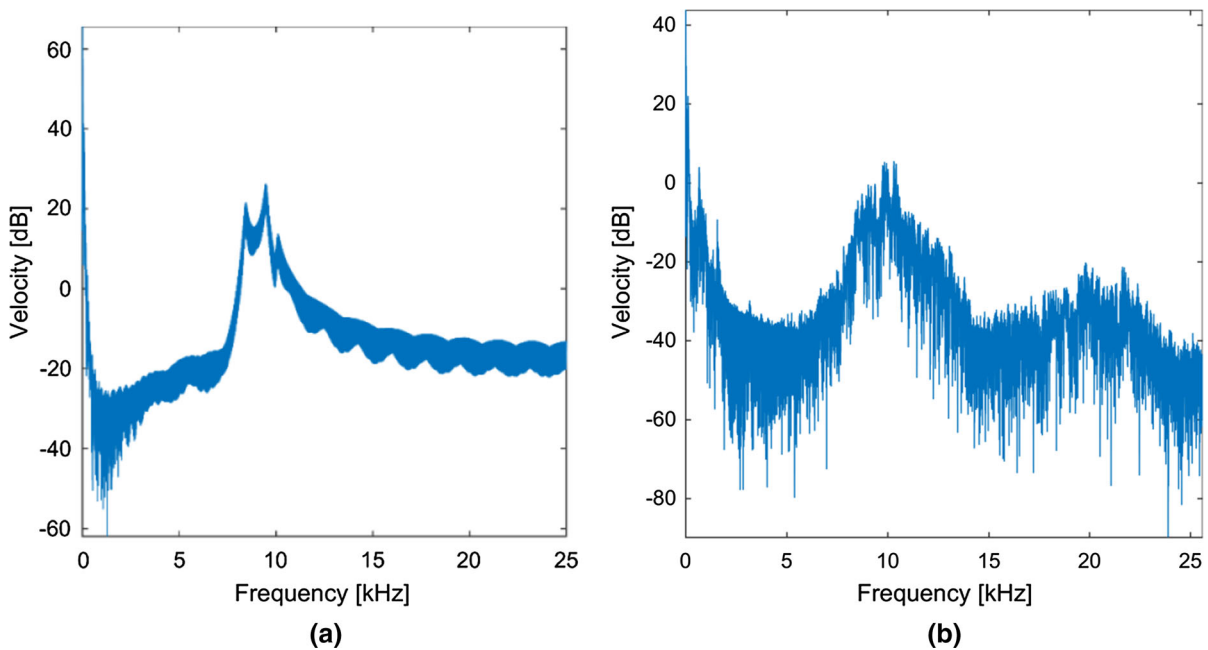


Fig. 17 Fourier transform of velocity signal from model (a) and experimental example (b) at time interval $t = 3-9$ s

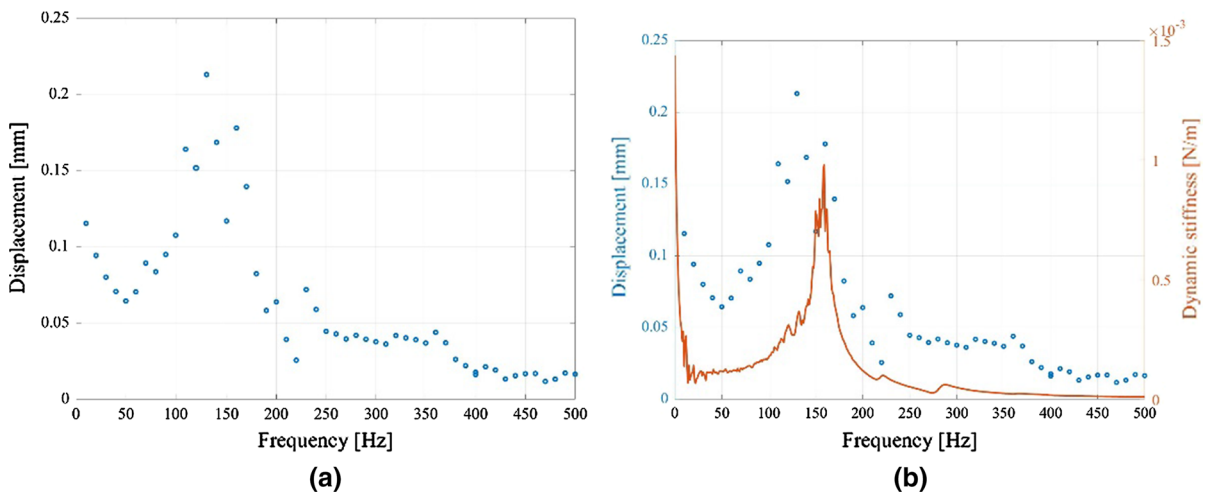


Fig. 18 Frequency characteristics of motion type changes (a), comparison with FRF for low frequencies (b)

tural components improves the quality of the model. In particular, this applies to the frequency domain. Further work assumes to consider high-frequency acoustic wave and observation of vibro-acoustic modulation effects.

Acknowledgements The work presented in this paper was performed within the scope of the research project 2015/17/B/ST8/03399 financed by the Polish National Science Centre.

Compliance with ethical standards

Conflict of interest The authors declare that they have no conflict of interest concerning the publication of this manuscript.

Open Access This article is distributed under the terms of the Creative Commons Attribution 4.0 International License (<http://creativecommons.org/licenses/by/4.0/>), which permits unrestricted use, distribution, and reproduction in any medium, provided you give appropriate credit to the original author(s) and

the source, provide a link to the Creative Commons license, and indicate if changes were made.

References

- Van Den Abeele, K., Le Bas, P.Y., Van Damme, B., Katkowski, T.: Quantification of material nonlinearity in relation to microdamage density using nonlinear reverberation spectroscopy: experimental and theoretical study. *J. Acoust. Soc. Am.* **126**(3), 963–972 (2009). <https://doi.org/10.1121/1.3184583>
- Klepka, A.: Nonlinear acoustics. In: *Advanced Structural Damage Detection: From Theory to Engineering Applications*, pp. 73–107 (2013). <https://doi.org/10.1002/9781118536148.ch4>
- Nazarov, V.E., Ostrovsky, L.A., Soustova, I.A., Sutin, A.M.: Nonlinear acoustics of micro-inhomogeneous media. *Phys. Earth Planet. Inter.* **50**(1), 65–73 (1988). [https://doi.org/10.1016/0031-9201\(88\)90094-5](https://doi.org/10.1016/0031-9201(88)90094-5)
- Klepka, A., Staszewski, W.J., Jenal, R.B., Szwedo, M., Iwaniec, J., Uhl, T.: Nonlinear acoustics for fatigue crack detection: experimental investigations of vibro-acoustic wave modulations. *Struct. Health Monit.* **11**(2), 197–211 (2012). <https://doi.org/10.1177/1475921711414236>
- Den Abeele, K.E.A.V., Carmeliet, J., Ten Cate, J.A., Johnson, P.A.: Nonlinear elastic wave spectroscopy (NEWS) techniques to discern material damage, part II: single-mode nonlinear resonance acoustic spectroscopy. *Res. Nondestruct. Eval.* **12**(1), 31–42 (2000). <https://doi.org/10.1080/09349840009409647>
- Klepka, A., Strączkiewicz, M., Pieczonka, L., et al.: Triple correlation for detection of damage-related nonlinearities in composite structures. *Nonlinear Dyn.* **81**(1–2), 453–468 (2015). <https://doi.org/10.1007/s11071-015-2004-6>
- Iwaniec, J., Uhl, T., Staszewski, W.J., Klepka, A.: Detection of changes in cracked aluminium plate determinism by recurrence analysis. *Nonlinear Dyn.* **70**(1), 125–140 (2012). <https://doi.org/10.1007/s11071-012-0436-9>
- Novak, A., Bentahar, M., Tournat, V., El Guerjouma, R., Simon, L.: Nonlinear acoustic characterization of micro-damaged materials through higher harmonic resonance analysis. *NDT E Int.* **45**(1), 1–8 (2012). <https://doi.org/10.1016/j.ndteint.2011.09.006>
- Korshak, B.A., Solodov, I.Y., Ballad, E.M.: DC effects, sub-harmonics, stochasticity and “memory” for contact acoustic non-linearity. *Ultrasonics* **40**, 707–713 (2002). [https://doi.org/10.1016/S0041-624X\(02\)00241-X](https://doi.org/10.1016/S0041-624X(02)00241-X)
- Broda, D., Pieczonka, L., Hiwarkar, V., Staszewski, W.J., Silberschmidt, V.V.: Generation of higher harmonics in longitudinal vibration of beams with breathing cracks. *J. Sound Vib.* **381**, 206–219 (2016). <https://doi.org/10.1016/j.jsv.2016.06.025>
- Guyer, R.A., Johnson, P.A.: *Nonlinear Mesoscopic Elasticity: The Complex Behaviour of Granular Media Including Rocks and Soil* (2009). <https://doi.org/10.1002/9783527628261>
- Naugolnykh, K.: Nonlinear acoustics: from research in physics to application (historical incidents). *Acoust. Phys.* **55**(3), 338–344 (2009). <https://doi.org/10.1134/S1063771009030087>
- Tournat, V., Gusev, V., Castagnède, B.: Non-destructive evaluation of micro-inhomogeneous solids by nonlinear acoustic methods. In: *Materials and Acoustics Handbook*, pp. 473–503 (2010). <https://doi.org/10.1002/9780470611609.ch18>
- Zaitsev, V.Y., Gusev, V., Castagnède, B.: Observation of the “Luxemburg–Gorky effect” for elastic waves. *Ultrasonics* **40**, 627–631 (2002). [https://doi.org/10.1016/S0041-624X\(02\)00187-7](https://doi.org/10.1016/S0041-624X(02)00187-7)
- Trojniar, T., Klepka, A., Pieczonka, L., Staszewski, W.J.: Fatigue crack detection using nonlinear vibro-acoustic cross-modulations based on the Luxemburg–Gorky effect. In: *SPIE Smart Structures and Materials + Nondestructive Evaluation and Health Monitoring*, p. 90641F-90641F-10 (2014)
- Pieczonka, L., Klepka, A., Martowicz, A., Staszewski, W.J.: Nonlinear vibroacoustic wave modulations for structural damage detection: an overview. *Opt. Eng.* **55**(1), 11005 (2015). <https://doi.org/10.1117/1.OE.55.1.011005>
- Pieczonka, L., Aymerich, F., Brozek, G., Szwedo, M., Staszewski, W.J., Uhl, T.: Modelling and numerical simulations of vibrothermography for impact damage detection in composites structures. *Struct. Control Health Monit.* **20**(4), 626–638 (2013). <https://doi.org/10.1002/stc.1483>
- Le Bas, P.Y., Remillieux, M.C., Pieczonka, L., Ten Cate, J.A., Anderson, B.E., Ulrich, T.J.: Damage imaging in a laminated composite plate using an air-coupled time reversal mirror. *Appl. Phys. Lett.* **107**(18), 184102 (2015). <https://doi.org/10.1063/1.4935210>
- Dittman, E., Adams, D.E.: Identification of cubic nonlinearity in disbonded aluminum honeycomb panels using single degree-of-freedom models. *Nonlinear Dyn.* **81**(1–2), 1–11 (2015). <https://doi.org/10.1007/s11071-015-1936-1>
- Klepka, A., Pieczonka, L., Staszewski, W.J., Aymerich, F.: Impact damage detection in laminated composites by non-linear vibro-acoustic wave modulations. *Compos. Part B Eng.* **65**, 99–108 (2014). <https://doi.org/10.1016/j.compositesb.2013.11.003>
- Fan, Y., Wang, H.: Nonlinear dynamics of matrix-cracked hybrid laminated plates containing carbon nanotube-reinforced composite layers resting on elastic foundations. *Nonlinear Dyn.* **84**(3), 1181–1199 (2016). <https://doi.org/10.1007/s11071-015-2562-7>
- Klepka, A., Staszewski, W.J., di Maio, D., Scarpa, F.: Impact damage detection in composite chiral sandwich panels using nonlinear vibro-acoustic modulations. *Smart Mater. Struct.* **22**(8), 84011 (2013). <https://doi.org/10.1088/0964-1726/22/8/084011>
- Bentahar, M., Marec, A., El Guerjouma, R., Thomas, J.H.: *Nonlinear Acoustic Fast and Slow Dynamics of Damaged Composite Materials: Correlation with Acoustic Emission*. Springer, Berlin (2009)
- Klepka, A., Staszewski, W.J., Uhl, T., Di Maio, D., Scarpa, F., Tee, K.F.: Impact Damage Detection in Composite Chiral Sandwich Panels, vol. 518 (2012). <https://doi.org/10.4028/www.scientific.net/KEM.518.160>
- Landau, L.D., Lifshitz, E.M.: *Theory of elasticity*, vol. 7 (1970). <http://cds.cern.ch/record/101816>
- Meo, M., Polimeno, U., Zumpano, G.: Detecting damage in composite material using nonlinear elastic wave spectroscopy methods. *Appl. Compos. Mater.* **15**(3), 115–126 (2008). <https://doi.org/10.1007/s10443-008-9061-7>

27. Pecorari, C.: Adhesion and nonlinear scattering by rough surfaces in contact: beyond the phenomenology of the Preisach-Mayergoyz framework. *J. Acoust. Soc. Am.* **116**(4), 1938 (2004). <https://doi.org/10.1121/1.1785616>
28. Solodov, I.Y.: Ultrasonics of non-linear contacts: propagation, reflection and NDE-applications. *Ultrasonics* **36**(1–5), 383–390 (1998). [https://doi.org/10.1016/S0041-624X\(97\)00041-3](https://doi.org/10.1016/S0041-624X(97)00041-3)
29. Zaitsev, V., Sas, P.: Dissipation in microinhomogeneous solids: inherent amplitude-dependent losses of a non-hysteretical and non-frictional type. *Acta Acust.* **86**, 429–445 (2000)
30. Moussatov, A., Gusev, V., Castagnede, B.: Self-induced hysteresis for nonlinear acoustic waves in cracked material. *Phys. Rev. Lett.* **90**(12), 124301/1–124301/4 (2003). <https://doi.org/10.1103/PhysRevLett.90.124301>
31. Duffour, P., Morbidini, M., Cawley, P.: A study of the vibro-acoustic modulation technique for the detection of cracks in metals. *J. Acoust. Soc. Am.* **119**(3), 1463–1475 (2006). <https://doi.org/10.1121/1.2161429>
32. Thompson, D.J.: The influence of the contact zone on the excitation of wheel/rail noise. *J. Sound Vib.* **267**, 523–535 (2003). [https://doi.org/10.1016/S0022-460X\(03\)00712-0](https://doi.org/10.1016/S0022-460X(03)00712-0)
33. Mohamed, M.A.S., Ahmadi, G., Loo, F.T.C.: Detection of asperity dynamic impacts on lightly loaded random surfaces. *Wear* **146**(2), 377–387 (1991). [https://doi.org/10.1016/0043-1648\(91\)90076-7](https://doi.org/10.1016/0043-1648(91)90076-7)
34. Slavič, J., Bryant, M.D., Boltežar, M.: A new approach to roughness-induced vibrations on a slider. *J. Sound Vib.* **306**(3–5), 732–750 (2007). <https://doi.org/10.1016/j.jsv.2007.06.036>
35. Solodov, I.: Nonlinear acoustic Ndt: approaches, methods, and applications. In: 10th International Conference of the Slovenian Society for Non-destructive Test, pp. 1–16 (2009). <http://www.ndt.net/article/Prague2009/ndtip/presentations/Solodov.pdf>. Accessed April 2010
36. Pecorari, C., Solodov, I.: Nonclassical nonlinear dynamics of solid surfaces in partial contact for NDE applications. In: Universality of Nonclassical Nonlinearity, pp. 309–326 (2006). https://doi.org/10.1007/978-0-387-35851-2_19
37. Feldmann, J.: Roughness-induced vibration caused by a tangential oscillating mass on a plate. *J. Vib. Acoust.* **134**(AUGUST), 1–9 (2012). <https://doi.org/10.1115/1.4005828>